Sciencexpress Report

Parallels Between Cytokinesis and Retroviral Budding: A Role for the ESCRT Machinery

Jez G. Carlton and Juan Martin-Serrano*

Department of Infectious Diseases, King's College London School of Medicine, London, UK.

*To whom correspondence should be addressed. E-mail: juan.martin_serrano@kcl.ac.uk

During cytokinesis, as dividing animal cells pull apart into two daughter cells, the final stage, termed abscission, requires breakage of the midbody, a thin membranous stalk connecting the daughter cells. This membrane fission event topologically resembles budding of viruses, such as HIV-1 from infected cells. Here we found that two proteins involved in HIV-1 budding--Tsg101, a subunit of the Endosomal Sorting Complex Required for Transport-I (ESCRT-I) and Alix, an ESCRT-associated protein--were recruited to the midbody during cytokinesis by interaction with Cep55, a centrosome and midbody-protein essential for abscission. Tsg101, Alix and possibly other components of ESCRT-I were required for completion of cytokinesis. Thus HIV-1 budding and cytokinesis utilize a similar subset of cellular components to carry out topologically similar membrane fission events.

Completion of cytokinesis requires the scission of a thin bridge of membrane connecting the daughter cells. The site of abscission is the midbody, a complex structure that contains proteins required for cell cleavage (*1*). Cytokinesis also requires dramatic remodelling of plasma membranes (*2*) and a number of vesicle trafficking components are thought to be involved in fusion events that precede abscission (*3–5*). The vesicle-tethering exocyst complex and two members of the SNARE machinery, namely syntaxin-2 and endobrevin/VAMP-8 (*6*, *7*), play an essential role in abscission, but it remains unclear whether SNARE-promoted fusion events are sufficient to complete the separation of the daughter cells. A topologically equivalent membrane scission event is needed to complete the last step of enveloped viruses egress. Retroviral late budding domains (L-domains) facilitate viral particle release from the infected cell by mediating a membrane fission event that separates the nascent virion from the plasma membrane (*8*). L-domains in HIV-1, Ebola virus and other enveloped viruses encode an essential PTAP motif which mediates its activity by recruiting Tsg101 (*9–11*). A second type of L-domain is encoded by the LYPxL motif, which facilitates retroviral egress by recruiting Alix (ALG-2-interacting protein X) a class E Vacuolar Protein Sorting (VPS) protein (*12–14*). Current models propose that ESCRT-III is the core machinery recruited by ESCRT-I and Alix to facilitate membrane fission (*15*), a function initially characterized in multivesicular body (MVB) formation.

Tsg101 preferentially localizes to late endosomal structures (*16*), although a cell cycle-dependent subcellular localization has been reported (*17*). To study Tsg101 localization in a physiological context, we replaced the endogenous protein by a monomeric Cherry (mCh, (*18*) fluorescent protein-Tsg101 fusion (mCh-Tsg101) expressed at endogenous levels in stable cells (Fig. 1A). Tsg101 activity in the mCh-Tsg101 cells was comparable to the parental HeLa cells as determined by HIV-1 virion release assays (Fig. 1A).

The most noticeable feature of mCh-Tsg101 was its localization to the midbody at late stages of cell division (Fig. 1B). Specifically, mCh-Tsg101 localized to the Flemming body, a phase-dense structure containing proteins involved in cell abscission (*6*). This localization led us to hypothesise that Tsg101 and perhaps other components of the ESCRT machinery might play a role in late stages of cytokinesis (Fig. 1C). A search for potential interactions with components of the cytokinesis machinery was performed by taking advantage of a proteome-scale map of human protein/protein interactions generated by yeast two-hybrid (*19*). Tsg101 was found to bind Cep55, a centrosomal protein that localizes to the midbody during late stages of cytokinesis required for abscission (*20*, *21*). The Tsg101-Cep55 interaction and Cep55 homo-multimerization activity were confirmed by yeast two-hybrid and co-precipitation assays (Fig. 1, D and E), suggesting that Tsg101 localization to the midbody might be mediated via interaction with Cep55. Indeed, depletion of Cep55 prevented Tsg101 recruitment to the midbody (Fig. 1B) and resulted in morphological abnormal Flemming bodies (*20*), confirming Cep55 suppression in these cells.

A subsequent screen against the human class E VPS pathway identified the interaction of Cep55 with Alix, a second protein required for retroviral egress (Fig. 1, D and E). The Cep55-Alix binding was confirmed by pull-down assays (Fig. 1E) and microscopy in cell lines stably expressing a

combination of YFP-Cep55 and either mCh-Tsg101 or mCh-Alix at near endogenous levels (Fig. 2 and fig. S1A). YFP-Cep55 localized to the midbody as described for the endogenous protein (*20*, *21*), and both mCh-Tsg101 and mCh-Alix colocalized with YFP-Cep55 in the central region of the midbody (Fig. 2A). Localisation of mCh-Alix to the midbody was also abolished in Cep55-depleted cells (fig. S1B).

We then employed RNAi to determine the role of Tsg101 and Alix in cytokinesis. In this assay, defects in cytokinesis are manifest by the appearance of multinucleated cells. Supporting an essential role in cytokinesis, depletion of Alix resulted in a 14-fold increase in the percentage of multinucleated cells compared with control cells (Fig. 2B). This phenotype was nearly identical to that observed upon depletion of Cep55 (*20*, *21*). Depletion of Tsg101 also resulted in an increased proportion of multinucleated cells (Fig. 2B), supporting the essential role of Tsg101 in abscission. Additionally, a marked toxicity was observed in cells depleted of Tsg101 (fig. S2A) (*22*), suggesting that cytokinetic defects may contribute to the reduced proliferative capacity and embryonic lethality observed in *tsg101* knockout embryos (*23*).

Thus, the cellular machineries involved in midbody abscission, MVB formation and retroviral budding share some components and are functionally related. To extend this notion, a dominant negative approach was followed taking advantage of VPS4, an AAA-ATPase that mediates disassembly and recycling of the ESCRT complexes from the endosomal membranes. Specifically, a catalytically inactive VPS4 (VPS4-DN) inhibits retroviral L-domain activity (*9*, *24*). We also followed a strategy whereby components of the ESCRT machinery exhibit a dominant negative effect when transiently overexpressed as fusions to heterologous proteins (*14*) and we used forms of Syntaxin-2 and Vamp-8 that lack transmembrane regions (STX2-δTM and Vamp8-δTM) and arrest cell division at late stages via inhibition of midbody abscission (*7*). Transfection of VPS4-DN induced an accumulation of multinucleated cells comparable to the effect of STX2-δTM and Vamp8-δTM (Fig. 2D). In contrast, these truncated SNAREs did not inhibit retroviral L-domain activity as determined by measuring infectious virus release (Fig. 2C). Furthermore, the overexpression of a YFP-Tsg101 fusion inhibited L-domain activity, presumably by disrupting the ESCRT-I stoichiometry, and a similar inhibition was observed in cell division (Fig. 2D). Similarly to HIV-1 budding (*14*), overexpression of CHMP4-ESCRT-III, but not ESCRT-II subunits, inhibited cytokinesis (fig. S2B). An analogous correlation between viral budding and cytokinesis was observed by overexpressing a YFP-Alix fusion, resulting in the inhibition of L-domain activity and cytokinesis (Fig. 2, C and D). Conversely, overexpression of Cep55, known to inhibit cytokinesis (*21*), also inhibited L-domain activity mediated by Tsg101 and Alix (Fig. 2C). Thus, L-domain activity and cytokinesis are closely related processes that share a requirement for key components of the ESCRT machinery. There are also important functional differences between both processes, as illustrated by the lack of inhibitory activity of the Syntaxin-2 and Vamp-8 deletions in retroviral budding.

The Cep55 binding site in Tsg101 was mapped to residues P_{158}-P-N-T-S_{162} in Tsg101's proline-rich region (fig. S3A). Deletion of residues 158-162 (Tsg101(δ158-162)) in full-length Tsg101 resulted in the loss of binding to Cep55, whereas binding of Tsg101(δ158-162) to other ESCRT-I components (VPS28 and VPS37A-D), viral (HIV-1 Gag, EbVP40) and endosomal proteins (Hrs, Tsg101, Alix and Tal) was unaffected (Fig. 3A). These results were confirmed by co-localization experiments. In transiently transfected cells, both YFP-Tsg101 and mCh-Cep55 exhibited a punctate distribution at interphase and localized to the Flemming body at late stages of cytokinesis (Fig. 3B). In both situations a nearly complete co-localization of Tsg101 and Cep55 was observed. In contrast, YFP-Tsg101(δ158-162) failed to colocalize with mCh-Cep55 despite displaying a punctate distribution in cells at interphase similar to that presented by wild type Tsg101 (Fig. 3B). More importantly, YFP-Tsg101(δ158-162) was not recruited to the midbody (Fig. 3B), suggesting that residues 158-162 in Tsg101 mediate its recruitment to the midbody by interacting with Cep55.

Thus, Cep55 is functionally linked to the ESCRT machinery via binding to Tsg101 and Alix. The budding inhibition by Cep55 overexpression confirmed this functional link but did not necessarily imply that Cep55 was required for L-domain activity. To address this issue, endogenous Tsg101 was depleted from 293T cells by siRNA and reintroduced by transfecting siRNA resistant plasmids with mutations in either the PTAP-binding site (M95A) (*25*) or in the Cep55-binding region (δ158-162). Depletion of Tsg101 results in a dramatic reduction of HIV-1 infectious particle release (Fig. 4A) (*9*) and the L-domain activity was rescued by transfecting a siRNA resistant Tsg101 but not with Tsg101(M95A). Similar experiments using Tsg101(δ158-162) showed that the Cep55 binding region in Tsg101 was not required for HIV-1 L-domain activity (Fig. 4A). Additionally, depletion of Cep55 had no effect on either Tsg101- or Alix-dependent budding (fig. S4), indicating that Cep55 is not required for L-domain activity.

We next determined the role of the Cep55-Tsg101 interaction in cytokinesis by following a similar depletion-replacement approach in HeLa cells. The percentage of multinucleated cells in Tsg101-depleted cells was restored to normal levels when the siRNA resistant Tsg101 was reintroduced, (Fig. 4B) showing that the cytokinesis defect

observed with the siRNA against Tsg101 was specific. An accumulation of cells arrested at the midbody stage was also observed in Tsg101-depleted cells (Fig. 4B) and midbody morphology was nearly identical to control cells, with formation of apparently normal Flemming bodies. Overall, the cytokinesis arrest observed in Tsg101-depleted cells is therefore consistent with defects in abscission. The replacement of Tsg101 mutants showed a partial cytokinesis defect in cells expressing Tsg101(δ158-162) and a similar partial phenotype was observed in Tsg101(M95A)-expressing cells (Fig. 4B), whereas a Tsg101 double mutant (M95A, δ158-162) recapitulated the phenotype of Tsg101-depleted cells (Fig. 4B). The effect of Tsg101(δ158-162) could be explained by lack of binding to Cep55 and recruitment to the midbody, but Tsg101(M95A) was recruited to the Flemming body (Fig. 4C), suggesting that a downstream defect might explain its phenotype. Alternatively, efficient Tsg101 recruitment to the midbody might occur in a complex with Alix and Cep55. Alix binds to the UEV domain of Tsg101 via a PSAP motif in the Proline Rich Region (PRR) and Tsg101(M95A) cannot bind Alix (*12*) while binding to other components of the ESCRT machinery remained unchanged (fig. S3). Thus, the partial phenotype observed with Tsg101(M95A) may indicate a requirement for the Tsg101-Alix interaction to complete abscission, although more work is needed to prove this point unequivocally. An additional requirement for other components of ESCRT-I, specifically VPS28, was strongly suggested by the phenotype observed in cells expressing Tsg101(A3), which does not bind VPS28 (*24*). Tsg101(A3) was recruited to the central region of the midbody (Fig. 4C) and the percentage of multinucleated cells induced by the A3 mutation fully accounted for the phenotype of Tsg101-depleted cells (Fig. 4B), suggesting that the Tsg101-VPS28 interaction is required to complete abscission.

In summary, we found that Cep55, a key component of the cellular machinery that mediates abscission, interacts with two endosomal proteins that facilitate retroviral budding, namely Tsg101 and Alix. The cellular pathways that mediate retroviral L-domain activity and abscission are closely interconnected, consistent with a model whereby the ESCRT machinery mediates membrane fission events essential for efficient separation of the daughter cells in the last step of cell division. The role of ESCRT complexes in yeast cytokinesis is unclear, but mutations in the Arabidopsis homologue of Tsg101 induce cytokinesis defects (*26*), suggesting that the role of the ESCRT machinery in abscission might be conserved in multicellular organisms.

References and Notes

1. U. S. Eggert, T. J. Mitchison, C. M. Field, *Annu. Rev. Biochem.* **75**, 543 (2006).
2. M. Glotzer, *Annu. Rev. Cell Dev. Biol.* **17**, 351 (2001).
3. V. Jantsch-Plunger, M. Glotzer, *Curr. Biol.* **9**, 738 (1999).
4. R. Albertson, B. Riggs, W. Sullivan, *Trends Cell Biol.* **15**, 92 (2005).
5. A. R. Skop, H. Liu, J. Yates, 3rd, B. J. Meyer, R. Heald, *Science* **305**, 61 (2004).
6. A. Gromley *et al.*, *Cell* **123**, 75 (2005).
7. S. H. Low *et al.*, *Dev. Cell* **4**, 753 (2003).
8. P. D. Bieniasz, *Virology* **344**, 55 (2006).
9. J. E. Garrus *et al.*, *Cell* **107**, 55 (2001).
10. J. Martin-Serrano, T. Zang, P. D. Bieniasz, *Nat. Med.* **7**, 1313 (2001).
11. L. VerPlank *et al.*, *Proc. Natl. Acad. Sci. U.S.A.* **98**, 7724 (2001).
12. U. K. von Schwedler *et al.*, *Cell* **114**, 701 (2003).
13. B. Strack, A. Calistri, S. Craig, E. Popova, H. G. Gottlinger, *Cell* **114**, 689 (2003).
14. J. Martin-Serrano, A. Yarovoy, D. Perez-Caballero, P. D. Bieniasz, *Proc. Natl. Acad. Sci. U.S.A.* **100**, 12414 (2003).
15. J. H. Hurley, S. D. Emr, *Annu. Rev. Biophys. Biomol. Struct.* **35**, 277 (2006).
16. S. Welsch *et al.*, *Traffic* **7**, 1551 (2006).
17. W. Xie, L. Li, S. N. Cohen, *Proc. Natl. Acad. Sci. U.S.A.* **95**, 1595 (1998).
18. N. C. Shaner *et al.*, *Nat. Biotechnol.* **22**, 1567 (2004).
19. J. F. Rual *et al.*, *Nature* **437**, 1173 (2005).
20. W. M. Zhao, A. Seki, G. Fang, *Mol. Biol. Cell* **17**, 3881 (2006).
21. M. Fabbro *et al.*, *Dev. Cell* **9**, 477 (2005).
22. A. Krempler, M. D. Henry, A. A. Triplett, K. U. Wagner, *J. Biol. Chem.* **277**, 43216 (2002).
23. J. Ruland *et al.*, *Proc. Natl. Acad. Sci. U.S.A.* **98**, 1859 (2001).
24. J. Martin-Serrano, T. Zang, P. D. Bieniasz, *J. Virol.* **77**, 4794 (2003).
25. O. Pornillos *et al.*, *EMBO J.* **21**, 2397 (2002).
26. C. Spitzer *et al.*, *Development* **133**, 4679 (2006).

27. We thank P. Bieniasz for stimulating discussions, M. Agromayor and M. Malim for critical reading of the manuscript, W. Sundquist and M. Malim for reagents. This work was supported by Career Establishment Grant G0400207 from the Medical Research Council UK. J.G.C. is a Beit Memorial Research Fellow.

Supporting Online Material

www.sciencemag.org/cgi/content/full/1143422/DC1

Materials and Methods

Figs. S1 to S4

References

4 April 2007; accepted 25 May 2007

Published online 7 June 2007; 10.1126/science.1143422

Include this information when citing this paper.

Fig. 1. Cep55 binds Tsg101 and Alix. (**A**) HeLa cells stably transduced with retroviral vectors expressing mCh or mCh-Tsg101. Cell lysates were analyzed with α-Tsg101 and α-Hsp90 antibodies. Tsg101 activity was determined by transfection with an HIV-1 proviral plasmid and analysis of cell lysates and extracellular virions by α-Gag immunoblotting. (**B**) Localization of mCh-Tsg101 in cells treated with the indicated siRNA. (**C**) Cartoon depicting conceptual similarities between viral budding and cytokinesis. (**D**) Cep55 fused to the VP16 activation domain was tested for interactions with the human class E VPS pathway by yeast two-hybrid. (**E**) Co-precipitation assay transfecting 293T cells with plasmids encoding GST or GST-Cep55 and either YFP-Cep55, YFP-Tsg101 or YFP-Alix. Cell lysates and glutathione-bound fractions were immunoblotted with an α-GFP antibody.

Fig. 2. Tsg101 and Alix are required for efficient completion of cytokinesis. (**A**) HeLa cells stably expressing both YFP-Cep55 and either mCh-Tsg101 or mCh-Alix were stained with α-tubulin and analyzed by confocal microscopy. (**B**) HeLa cells were transfected with siRNA targeting Cep55, Tsg101 or Alix, fixed, stained with α-tubulin and scored for multinucleation (n = 5 ± SD). Representative micrograghs given, arrows indicate cells at midbody stage. Cell lysates were normalised for Hsp90 levels and immunoblotted with anti-Tsg101, anti-Cep55, anti-Alix or anti-Hsp90 antisera. (**C**) 293T cells were transiently transfected with plasmids encoding YFP-tagged fusion proteins and pNL/HXB HIV-1 provirus. Cell lysates and virions were examined by immunoblotting with α-Gag antisera. β-Galactosidase assay was performed upon HeLa-TZM-bl cells infected with 293T supernatant (n = 4 ± SD). (**D**) HeLa cells transfected with plasmids encoding YFP-tagged fusion proteins were fixed, stained with α-tubulin and scored for multinucleated cells (n = 3 ± SD). Representative micrograghs given.

Fig. 3. Residues 158PPNTS162 in the Proline-rich domain of Tsg101 co-ordinate Cep55. (**A**) Tsg101 or Tsg101(δ158-162) fused to the Gal4 DNA-binding domain were tested for interaction with a variety of Tsg101-interacting proteins fused to the VP16 activation domain via yeast 2-hybrid assay. (**B**) HeLa cells transiently transfected with plasmids encoding mCh-Cep55 and either YFP-Tsg101 or YFP-Tsg101(δ158-162) were fixed and stained with α-tubulin.

Fig. 4. The Tsg101-Cep55 interaction is required for cytokinesis, but not for viral budding. (**A**) 293T cells were treated with siRNA targeting Luciferase or Tsg101. pNL/HXB HIV-1 provirus and YFP or siRNA-resistant YFP-Tsg101 encoding plasmids were included in the second transfection. 293T lysates were examined by immunoblotting with α-GFP antisera. Lysates and virions were examined with anti-Gag antisera. β-Galactosidase assay was performed upon HeLa-TZM-bl reporter cells infected with 293T supernatant. (**B**) Stably transduced HeLa cells expressing mCh or the indicated siRNA resistant mCh-Tsg101 plasmids were treated with the indicated siRNA. Cells were fixed, stained with α-tubulin and scored for multinucleation or arrest at midbody (n = 5 ± SD). Cell lysates were examined by immunoblotting with α–Tsg101 or -Hsp90 antisera. (**C**) Representative micrographs describing midbody localisation of mCh or mCh-Tsg101 mutants in dividing cells.

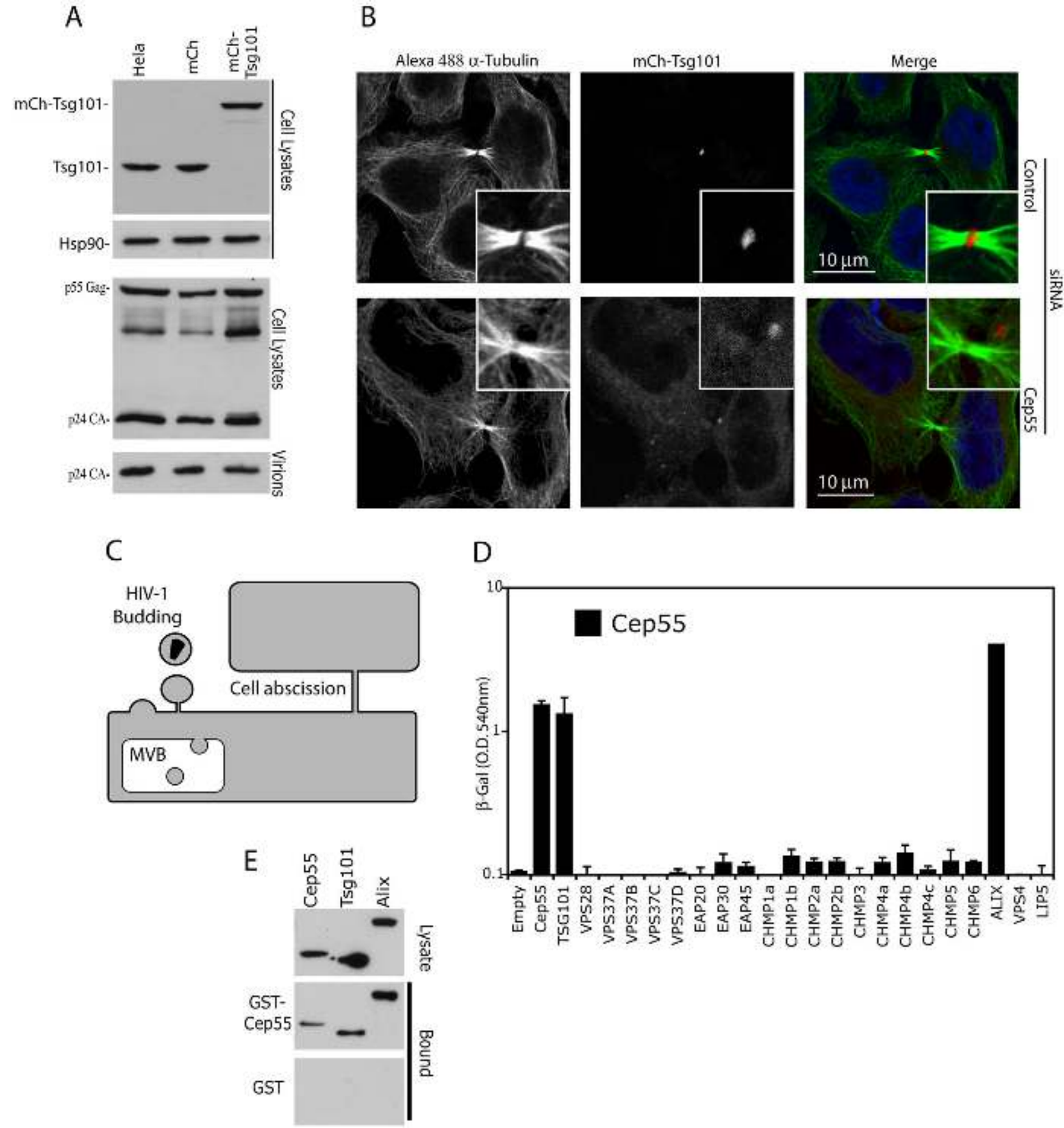
A
Hela
mCh
mCh-Tsg101
mCh-Tsg101-
Tsg101-
Hsp90-
Cell Lysates
p55 Gag-
p24 CA-
Cell Lysates
p24 CA-
Virions
B
Alexa 488 α-Tubulin
mCh-Tsg101
Merge
Control
siRNA
Cep55
10 μm
10 μm
C
HIV-1
Budding
Cell abscission
MVB
D
Cep55
β-Gal (O.D.540nm)
10
1
0.1
Empty
Cep55
TSG101
VPS28
VPS37A
VPS37B
VPS37C
VPS37D
EAP20
EAP30
EAP45
CHMP1a
CHMP1b
CHMP2a
CHMP2b
CHMP3
CHMP4a
CHMP4b
CHMP4c
CHMP5
CHMP6
ALIX
VPS4
LIP5
E
Cep55
Tsg101
Alix
Lysate
GST-
Cep55
GST
Bound

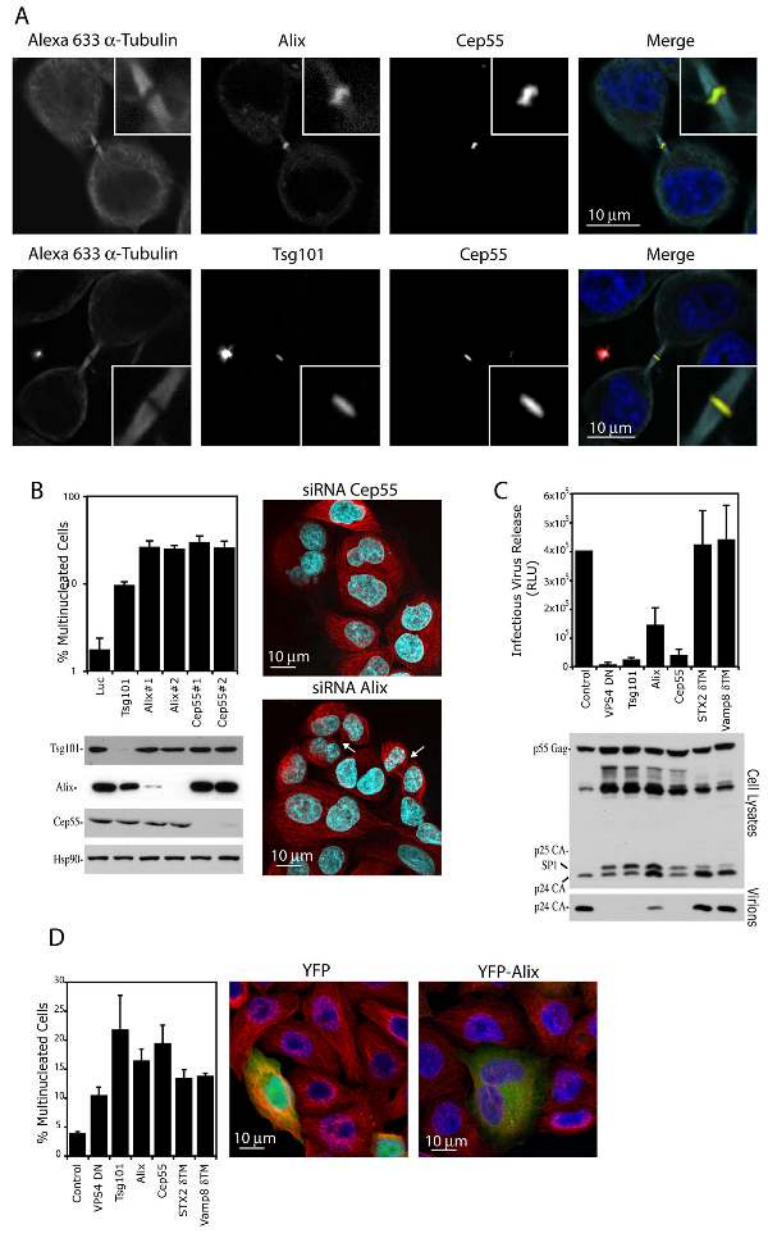
A
Alexa 633 α-Tubulin
Alix
Cep55
Merge
10 µm
Alexa 633 α-Tubulin
Tsg101
Cep55
Merge
10 µm
B
% Multinucleated Cells
Luc
Tsg101
Alix#1
Alix#2
Cep55#1
Cep55#2
Tsg101
Alix
Cep55
Hsp90
siRNA Cep55
10 µm
siRNA Alix
10 µm
C
Infectious Virus Release (RLU)
Control
VPS4 DN
Tsg101
Alix
Cep55
STX2 ΔTM
Vamp8 ΔTM
p55 Gag
p25 CA-SP1
p24 CA
p24 CA
Cell Lysates
Virions
D
% Multinucleated Cells
Control
VPS4 DN
Tsg101
Alix
Cep55
STX2 ΔTM
Vamp8 ΔTM
YFP
10 µm
YFP-Alix
10 µm

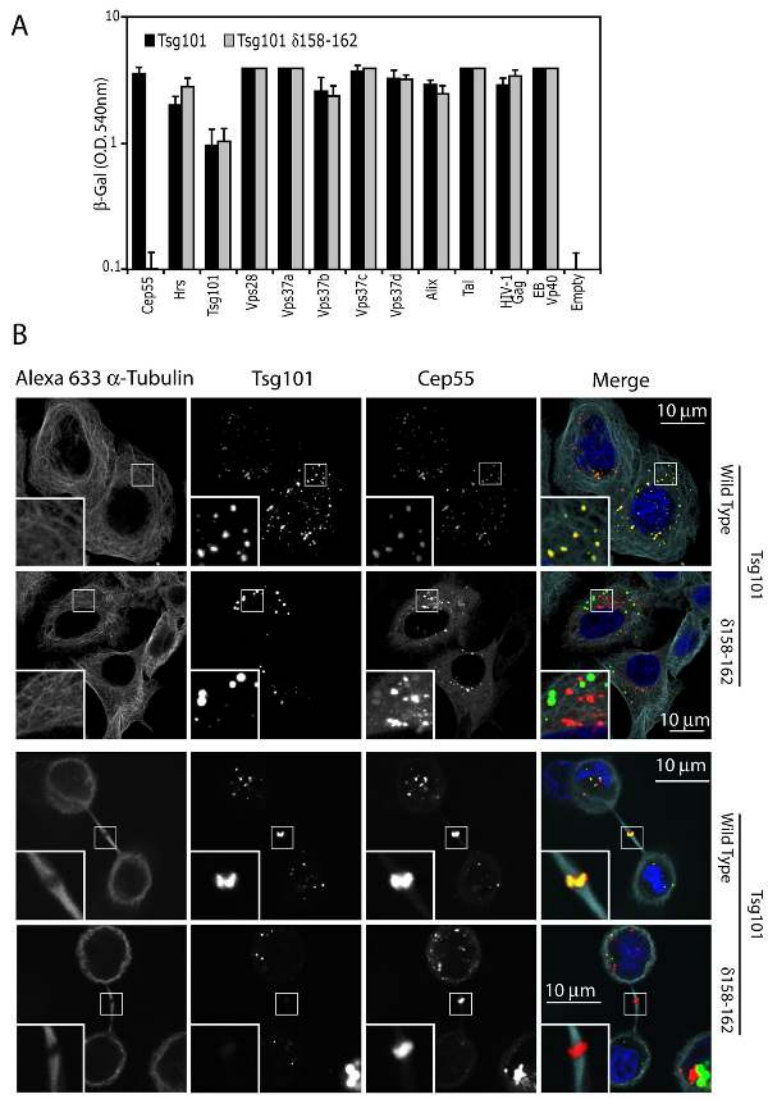
A
Tsg101
Tsg101 δ158-162
β-Gal (O.D.540nm)
10
1
0.1
Cep55
Hrs
Tsg101
Vps28
Vps37a
Vps37b
Vps37c
Vps37d
Alix
Tal
HIV-1 Gag
EB Vp40
Empty
B
Alexa 633 α-Tubulin
Tsg101
Cep55
Merge
10 μm
Wild Type
δ158-162
Tsg101

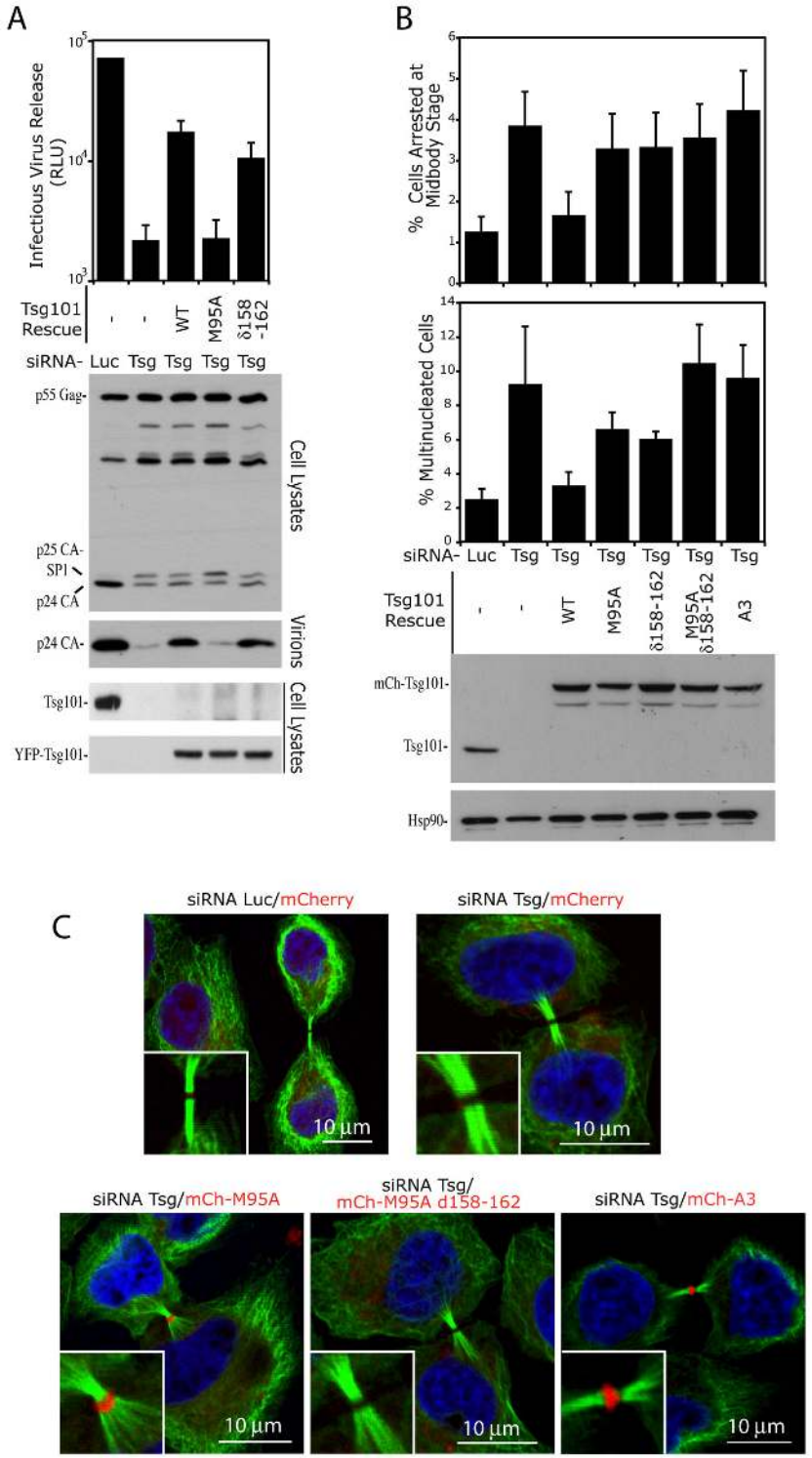
A
Infectious Virus Release (RLU)
Tsg101 Rescue
-
-
WT
M95A
δ158 -162
siRNA- Luc Tsg Tsg Tsg Tsg
p55 Gag-
p25 CA-
SPI
p24 CA
Cell Lysates
p24 CA-
Virions
Tsg101-
Cell Lysates
YFP-Tsg101-
B
% Cells Arrested at Midbody Stage
% Multinucleated Cells
siRNA- Luc Tsg Tsg Tsg Tsg Tsg Tsg
Tsg101 Rescue
-
-
WT
M95A
δ158-162
M95A δ158-162
A3
mCh-Tsg101-
Tsg101-
Hsp90-
C
siRNA Luc/mCherry
siRNA Tsg/mCherry
siRNA Tsg/mCh-M95A
siRNA Tsg/ mCh-M95A d158-162
siRNA Tsg/mCh-A3
10 µm

www.sciencemag.org/cgi/content/full/1143422/DC1

Supporting Online Material for

Parallels Between Cytokinesis and Retroviral Budding: A Role for the ESCRT Machinery

Jez G. Carlton and Juan Martin-Serrano*

*To whom correspondence should be addressed. E-mail: juan.martin_serrano@kcl.ac.uk

Published 7 June 2007 on *Science* Express

DOI: 10.1126/science.1143422

This PDF file includes:

SUPPLEMENTARY ONLINE MATERIAL

MATERIALS AND METHODS

Antibodies

Monoclonal anti-Tsg101 (4A10) was from Abcam, polyclonal anti-Cep55 (A01) was from Abnova, polyclonal HSP90 (H114) was from Santa Cruz Biotechnology, monoclonal anti-α-Tubulin (DM1a) was from Sigma, monoclonal anti-p24 Gag (183-H12-5C) was produced in house. Monoclonal anti-GFP (7.1/13.1) was from Roche. Polyclonal anti-Alix was a kind gift from Prof. W. Sundquist. Alexa- and HRP-conjugated secondary antibodies were from Molecular Probes and Cell Signalling Technology respectively.

Plasmids

Cep55 was PCR-amplified from IMAGE clone 3028566 using primers Fwd 5'-ATATGAATTCATGTCTTCCAGAAGTACC-3' and Rev 5'-ATATCTCGAGCTACTTTGAACAGTATTCC-3' and cloned EcoRI-XhoI into a modified pCR3.1 containing a YFP-EcoRI-XhoI-NotI polylinker in place of its multiple cloning site (MCS). All subsequent constructs were generated by transfer of the EcoRI-Cep55-XhoI cassette into vectors whose MCS had previously been replaced with an EcoRI-XhoI-NotI polylinker. Truncations and deletions of Tsg101 or were created using PCR-based methodologies; in the case of deletions, a HindIII site was inserted in place of

the indicated residues. siRNA resistant forms of Tsg101 were created by subcloning an EcoRI-SphI fragment of Tsg101 1-250 containing silent mutations 138EPPVFSR144 (generated by mutagenic PCR with Fwd : GTATTTGGAGATGAGCCGCCGGTGTTTAGCAGACCTATTTCGGCATCC and Rev : GGATGCCGAAATAGGTCTGCTAAACACCGGCGGCTCATCTCCAAATAC primers) into the EcoRI and SphI sites of wildtype or mutated forms of pCR3.1-YFP-Tsg101. Residues 1-234 of Syntaxin-2 were PCR-amplified from IMAGE clone 5296500 using primers Fwd 5'- ATATGAATTCATGCGGGACCGGCTGC-3': and Rev : 5'-ATATCTCGAGTCTTTCTATGTTGTTGATCATTTCACC-3'and cloned EcoRI-XhoI into pCR3.1-YFP-EcoRI-XhoI-NotI. Residues 1-75 of Vamp8/endobrevin were PCR-amplified from IMAGE clone 3538672 using primers Fwd : 5'-ATATGAATTCATGGAGGAAGCCAGTGAAGGTGGAGG-3' and Rev : 5'-ATATCTCGAGCTTCACGTTCTTCCACCAGAATTTCCG-3' and cloned EcoRI-XhoI into pCR3.1-YFP-EcoRI-XhoI-NotI. All other constructs have been previously described (*S1,S2,S3*) and where necessary, were subcloned as required.

Transient transfection

HeLa cells were transfected using Lipofectamine-2000 (Life Technologies) according to the manufacturers instructions. 293T cells were transfected using linear 25-kDa polyethylenimine (PEI, Polysciences, Inc.) by combining 1 μg of plasmid DNA with 4 μl of PEI (1 mg/ml) in 50 μl of serum free DMEM for 15 minutes prior to addition to cells.

siRNA transfections

Cells were seeded at a density of 1E5 cells/ml (HeLa) or 2.6E5 cells/ml (293T) and were transfected 2 hours after plating with siRNA targeting either Luciferase (Control: CUGCCUGCGUGAGAUUCUC), Tsg101 (CCUCCAGUCUUCUCUCGUC, (*S4*)), Alix (1 : GAAGGAUGCUUUCGAUAAAUU, 2 : GCAGUGAGGUUGUAAAUGU) or Cep55 (1 : GGAGAAGAAUGCUUAUCAA, 2 : GAAGAGAAUGAUAUUGCUA) at 100nM concentration using Dharmafect-1 (Dharmacon). After 48 hours, cells were reseeded and transfected again with siRNA using Dharmafect-1, or with siRNA and DNA using Lipofectamine-2000. 48 hours later, cells were assayed.

Virus budding and infectivity assays

293T cells were co-transfected with 300 ng of pCR3.1-YFP-fusion protein encoding plasmid and 300 ng of pNL/HXB HIV-1 provirus for 48 hours. For siRNA experiments, 293T cells were transfected with siRNA as described above, except that the second transfection contained additionally either 300 ng of HIV-1 pNL/HXB provirus or 300 ng HIV-1 pNL/HXB lacking the p6 L-domain and 200 ng of a plasmid expressing a truncated HIV-1 pNL/HXB-Gag protein fused to either the p6 L-domain of HIV-1 or the p9 L-domain of EIAV. For siRNA rescue experiments, 2 ng of plasmid encoding YFP or siRNA resistant YFP-Tsg101, YFP-Tsg101(M95A) or YFP-Tsg101(δ158-162) was included. After 48 hours, virions were harvested from 293T supernatants by filtration (0.2 μm) and centrifugation through 20% sucrose (14000 rpm, 120 minutes), lysed, resolved by SDS-PAGE and examined by western blotting. Additionally, HeLa-TZM-bl cells (CD4+, CXCR4+, CCR5+, HIV-1 LTR-LacZ) (*S5*) were infected with 1 μl of NL/HXB supernatant or 50 μl of NL/HXB-p6 or NL/HXB-p9 supernatant for 48 hours. *LacZ*

activities in cell lysates were measured by chemiluminescent detection of β-Galactosidase using Galacto-Star (Applied Biosystems).

Generation of stable cell lines

293T cells were transfected with 100 ng of pHIT-VSVG, 700 ng of MLV-GagPol and 200 ng of a retroviral packaging vector encoding cDNAs of interest for 48 hours. Cep55 was cloned as an N-terminal YFP fusion into pMSCVneo-YFP-EcoRI-XhoI-NotI, a retroviral packaging vector encoding a neomycin resistance gene. Tsg101 and Alix were cloned as N-terminal mCh fusions into pCMS28-mCh-EcoRI-NotI-XhoI (A modified gift from Prof. Mike Malim), a bi-cistronic retroviral packaging vector encoding a puromycin resistance gene linked via an IRES to the MCS. siRNA resistant Tsg101 mutants were similarly cloned into pCMS28 mCh-EcoRI-NotI-XhoI. 293T supernatants were filtered (0.2 μm) and used to transduce HeLa cells. Selection with puromycin (200 ng/ml) or neomycin (500 μg/ml) was applied as required 24 hours later and cells were passaged under continual selection. In the case of mCh-Tsg101 and mutants thereof, replacement of endogenous Tsg101 occurs by a compensatory post-transcriptional down regulation of Tsg101 induced by a sustained over-expression of the exogenous Tsg101 (S6). To create doubly stable HeLa cell lines of YFP-Cep55 and mCh-Tsg101 or mCh-Alix, a clonal HeLa-YFP-Cep55 cell line was obtained by limiting dilution, prior to transduction with pCMS28-mCh-Tsg101 or pCMS28-mCh-Alix containing virus.

Imaging

HeLa cells were seeded onto glass coverslips 24 hours previous and were fixed with 3% paraformaldehyde for 15 minutes. Cells were permeabilised with PBS 0.1% Tx100 for 5 minutes and treated sequentially with PBS 100 mM glycine for 30 minutes, PBS 1% BSA for 30 minutes, then stained with primary antibodies in PBS 1% BSA for 2 hours. Alexa488, Alexa594 or Alexa633 conjugated secondary antibodies were applied in PBS for 1 hour. Nuclei were visualised using Hoechst 33258 and coverslips were mounted in Mowiol. Slides were imaged using a Leica AOBS SP2 confocal microscope, employing the AOTF to collect relevant narrow emission-λ windows for each flurophore. Geryscale images were pseudocoloured and combined in Photoshop (Adobe) to create the merged images.

Yeast Two-Hybrid assays

Yeast Y190 cells were co-transformed with plasmids encoding the indicated proteins fused to the VP16 activation domain (pHB18) or the Gal4 DNA-binding domain (pGBKT7). Co-transformants were selected on SD-Leu-Trp agar for 3 days at 30 ^{o}C, harvested, and *LacZ* activity was measured using a liquid β-galactosidase assay employing chlorophenolred-ß-D-galactopyranoside (Roche) as a substrate.

Co-precipitation Assays

Cep55 was cloned as a GST-fusion into the EcoRI and XhoI sites of pCAGGS/GST-EcoRI-NotI-XhoI. 293T cells were co-transformed with 2 ug of either pCAGGS/GST or pCAGGS/GSTCep55 and 2 ug of pCR3.1-YFP, pCR3.1-YFP-Tsg101 or pCR3.1-YFP-Alix for 48 hours. cells were harvested and lysed in 1 ml of 50 mM Tris·HCl, pH 7.4, 150

mM NaCl, 5 mM EDTA, 5% glycerol, 1% Triton X-100, and a protease inhibitor mixture (complete mini-EDTA-free, Roche Applied Science). Clarified lysates were incubated with glutathione-Sepharose beads (Amersham Biosciences) for 3 h at 4 °C and washed three times with wash buffer (50 mM Tris·HCl, pH 7.4, 150 mM NaCl, 5 mM EDTA, 5% glycerol, 0.1% Triton X-100). Bead-bound proteins were resolved by SDS-PAGE and examined by western blotting.

Multinucleation Assays.

HeLa cells were transfected with 400 - 500 ng of pCR3.1-YFP fusion proteins for 48 hours, (cells were re-seeded onto glass coverslips after 24 hours). Additionally, 50 ng of pCR3.1-YFP was included with YFP-Vps4DN to facilitate identification of transfected cells. Alternatively, cells were transfected with the indicated siRNA for 48 hours, re-seeded onto glass coverslips and re-transfected with siRNA for 48 hours if required. Cells were then fixed and were identified through α-tubulin staining. 100 cells per coverslip were scored for presence of more than one nucleus in overexpression assays. For ESCRT-II and ESCRT-III overexpression, well-adhered non-apoptotic cells were selected. 300 cells per coverslip were scored for presence of more than one nucleus in siRNA assays. In all cases, cells unambiguously connected by midbodies were considered multinucleated.

Viability Assays

Detached cells were collected by centrifugation and resuspended in SF-DMEM. Trypan-blue was added to a final concentration of 0.06% and cells were scored for trypan-blue

exclusion using a haemocytomoter. Cell counts were normalised against the total cell number obtained for HeLa-mCh cells treated with luciferase siRNA.

SUPPLEMENTARY FIGURE LEGENDS

Figure S1 : (A) Doubly-stable cell lines generated by sequential transduction with retroviruses encoding YFP-Cep55 and either mCh-Alix or mCh-Tsg101 express these proteins at near endogenous levels. Indicated HeLa cell lines were lysed, resolved by SDS-PAGE and examined by immuno-blotting with α-Tsg101, α-Alix, α-Cep55 or α–Hsp90 antisera. (B) Cep55 siRNA prevents Alix recruitment to the midbody. (B) Stably transduced HeLa cells expressing mCh-Alix were treated with the indicated siRNA, stained against α-tubulin and examined by confocal microscopy.

Figure S2 : (A) Loss of Tsg101 results in cellular toxicity. Stably transduced HeLa cells expressing mCh, or siRNA resistant mCh-Tsg101 were treated with siRNA targeting luciferase or Tsg101. Cell viability was assessed by trypan blue exclusion. Similar toxicity was observed in untransduced HeLa cells. (B) ESCRT-III, but not ESCRT-II overexpression disrupts cytokinesis. Hela cells were transiently transfected with plasmids encoding YFP, YFP-Tsg101, -Eap20, -Eap30, -Eap45, -Chmp4a, -Chmp4b or –Chmp4c, fixed, stained against α-tubulin and examined by confocal microscopy.

α-tubulin and examined by confocal microscopy.

Figure S3 : Analysis of Tsg101 interactions by yeast 2-hybrid assay. (A) The indicated Tsg101 truncations or deletions were fused to the Gal4 DNA-binding domain and tested for interaction with Cep55 fused to the VP16 activation domain by yeast 2-hybrid assay. (B) Tsg101 or Tsg101(M95A) were fused to the Gal4 DNA-binding domain and tested for interaction a variety of Tsg101-interacting proteins fused to the VP16 activation domain by yeast 2-hybrid assay.

Figure S4 : Cep55 is not required for HIV-1 p6-dependent or EIAV p9-dependet virus budding. (A) 293T cells were treated with the indicated siRNA. For the second transfection, a pNL/HXBδp6 plasmid lacking the entire p6 late domain and a plasmid encoding pNL/HXB-Gag fused to either the p6 L-domain of HIV-1-Gag or the p9 L-domain of EIAV-Gag were combined with the siRNA oligos. After 48 hours, cell lysates and released virions were resolved by SDS-PAGE and examined by western blotting with α-Gag antisera. Cell lysates were also examined by western blotting with α-Tsg101, α-Cep55, α-Alix and α-Hsp90 antisera. β-Galactosidase assay was performed upon HeLa-TZM-bl cells infected with 293T supernatant for 48 hours.

SUPPLEMENTARY REFERENCES

S1. J. Martin-Serrano, A.Yarovoy, D. Perez-Caballero, P.D. Bieniasz, *Proc. Nat. Acad. Sci.* **100**, 12419 (2003).

S2. J. Martin-Serrano, T. Zang, P.D. Bieneisz, *Nat. Med*. **7**, 1313 (2001).

S3. J. Martin-Serrano, T. Zang, P.D. Bieneisz, *J Virol*. **77,** 4794 (2003).

S4. J. E. Garrus *et al.*, *Cell* **107**, 55 (2001).

S5. C. A. Derdeyn *et al*., *J. Virol*. **74**, 8358 (2000).

S6. G. H. Feng, C. J. Lih, S. N. Cohen, *Cancer Res* **60**, 1736 (2000).

Figure S1

A

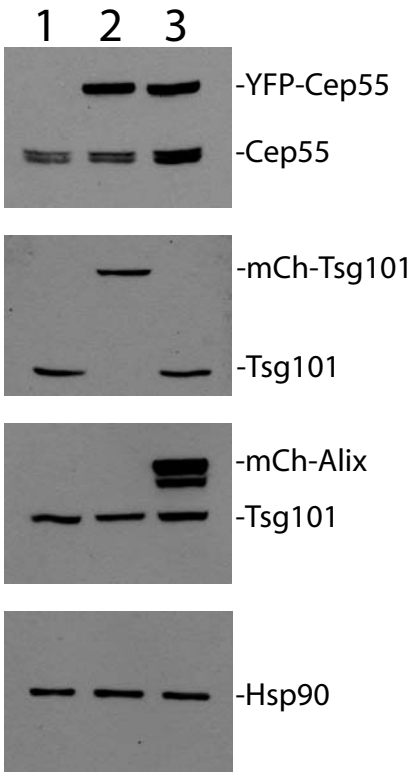

1- Hela
2- Hela YFP-Cep55+ mCh-Tsg101
3- Hela YFP-Cep55+ mCh-Alix

B

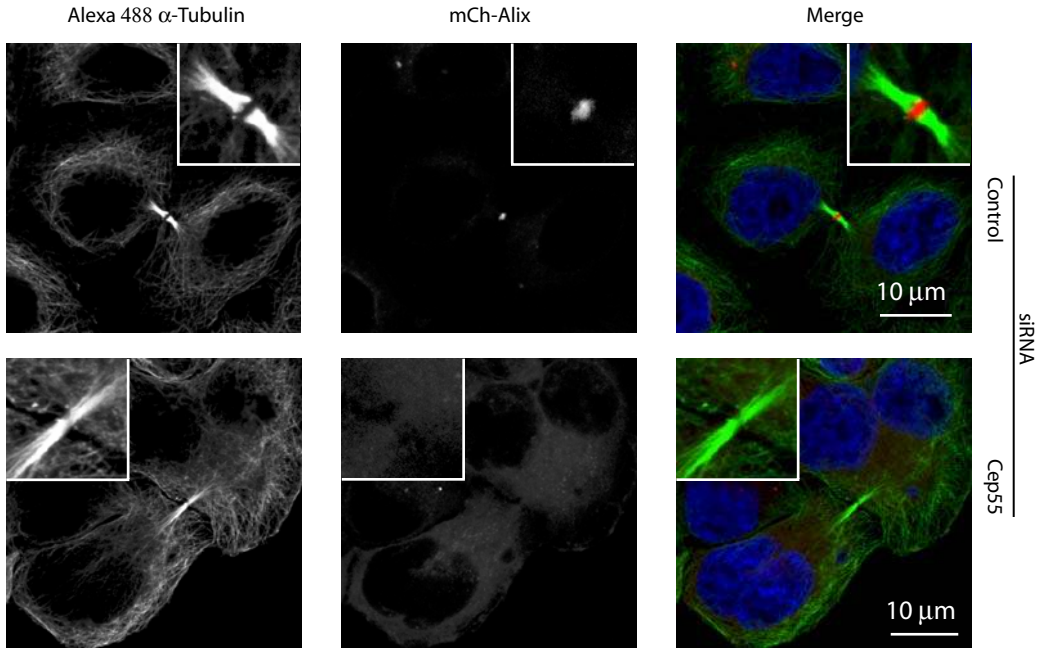

A

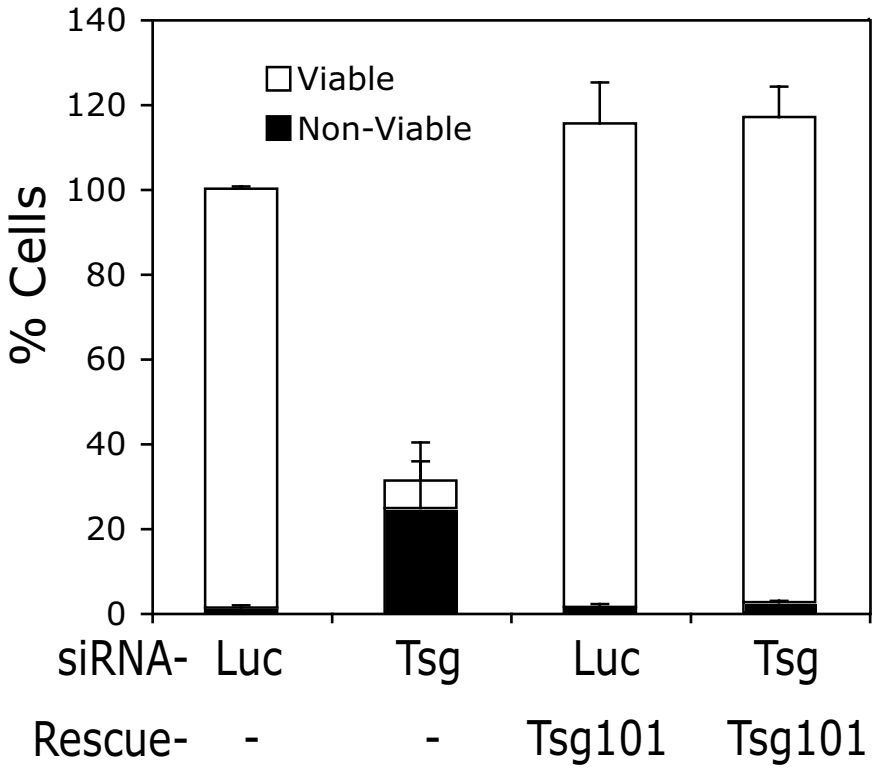
140
120
100
80
60
40
20
0
% Cells
Viable
Non-Viable
siRNA- Luc Tsg Luc Tsg
Rescue- - - Tsg101 Tsg101

B

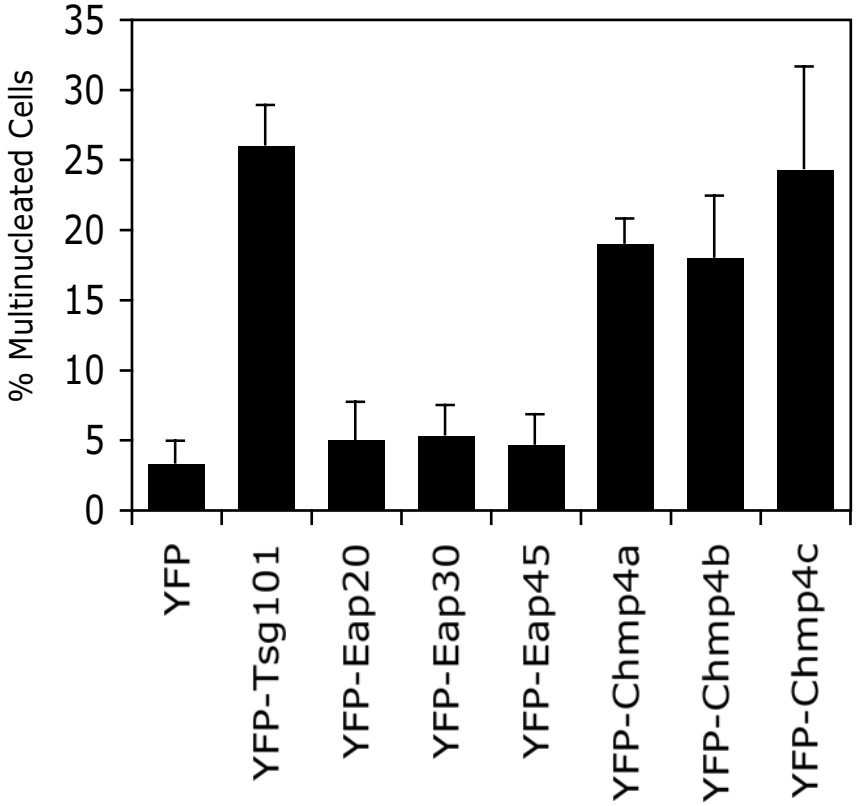
35
30
25
20
15
10
5
0
% Multinucleated Cells
YFP
YFP-Tsg101
YFP-Eap20
YFP-Eap30
YFP-Eap45
YFP-Chmp4a
YFP-Chmp4b
YFP-Chmp4c

Figure S3

A

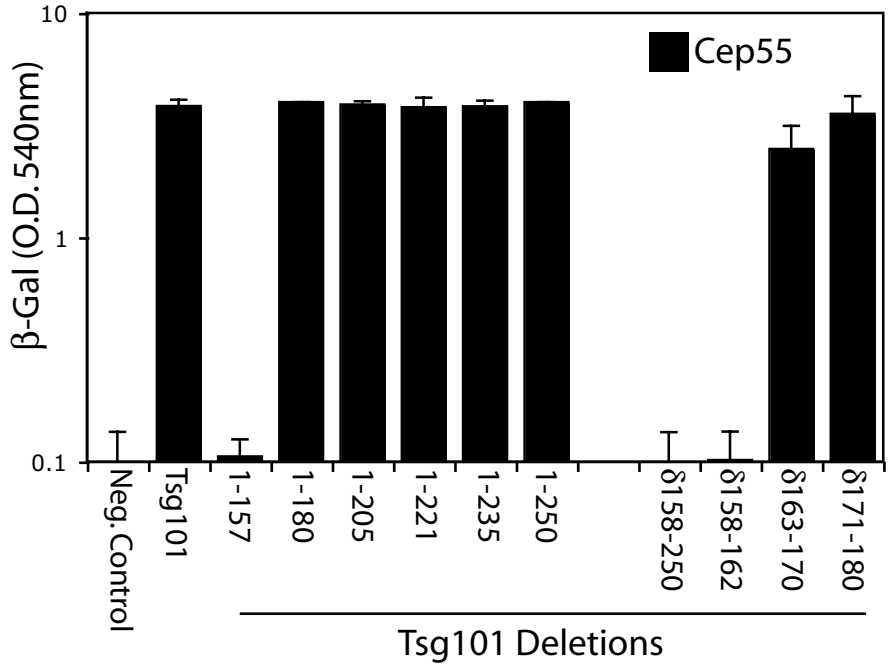
Cep55
β-Gal (O.D. 540nm)
10
1
0.1
Neg. Control
Tsg101
1-157
1-180
1-205
1-221
1-235
1-250
δ158-250
δ158-162
δ163-170
δ171-180
Tsg101 Deletions

B

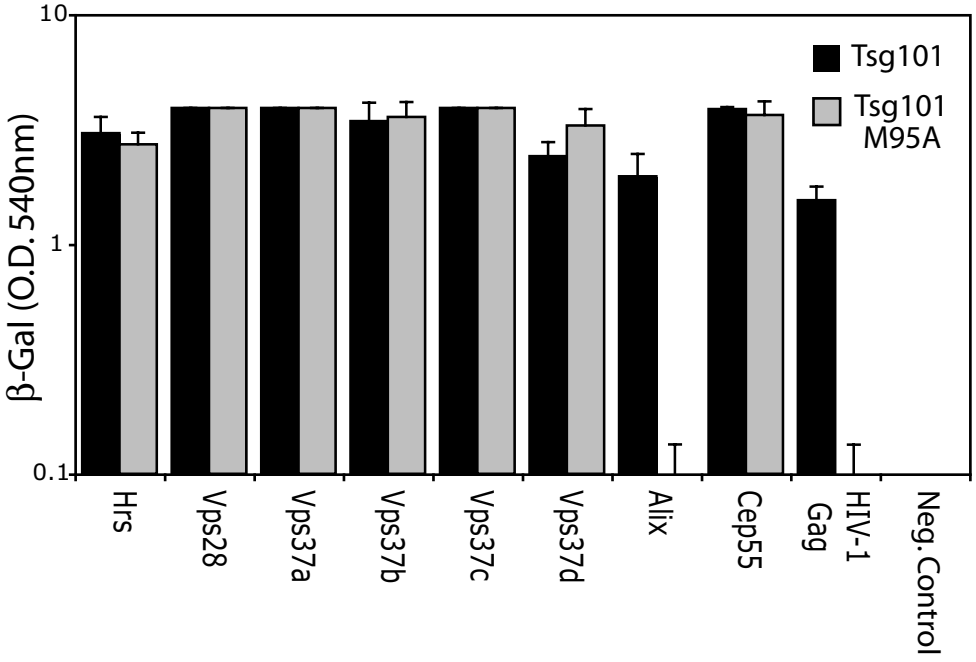
Tsg101
Tsg101 M95A
β-Gal (O.D. 540nm)
10
1
0.1
Hrs
Vps28
Vps37a
Vps37b
Vps37c
Vps37d
Alix
Cep55
HIV-1 Gag
Neg. Control

Figure S4

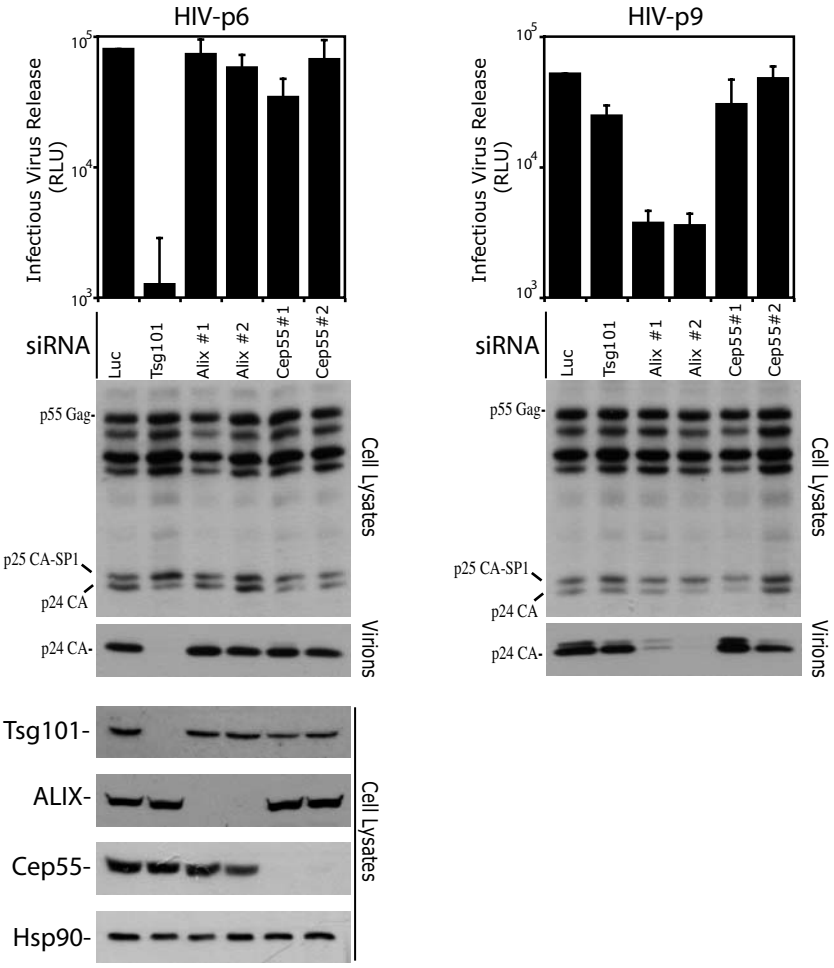
HIV-p6
HIV-p9
Infectious Virus Release (RLU)
siRNA
Luc
Tsg101
Alix #1
Alix #2
Cep55#1
Cep55#2
p55 Gag-
p25 CA-SP1
p24 CA
p24 CA-
Cell Lysates
Virions
Tsg101-
ALIX-
Cep55-
Hsp90-